Koopman Modeling of Human Gait Dynamics for Global Modal Analysis Using Periodic Motion Regularization

Emily Kamienski[1] *Graduate Student Member, IEEE*, Seth Donahue[2], Matthew J. Major[3], and H. Harry Asada[1]*Life Fellow, IEEE*

***Abstract*— This paper presents a data driven global linear model of steady state walking dynamics. Instantaneous whole body angular momentum is a physics informed aggregate quantity used as a marker for dynamic balance during locomotion. Gait dynamics are often modeled as hybrid and nonlinear. We propose using Koopman Operators to model the gait stability dynamics with a global, linear model. This is achieved by augmenting the whole body angular momentum state variables with learned observables, or basis functions, such that the dynamics look linear in the lifted dimension. Considering that the gait dynamics are periodic, a regularization term that encourages the state transition matrix to be orthonormal is added to the loss term when learning the observables. This forces a periodic model to be learned and prevents the likelihood of unstable poles. A low average MSE was obtained over 2 gait cycles for different population types, each with slightly differing gait dynamics. Furthermore, this linear representation enables the use of linear analysis tools that could have clinical implications for assessing the gait of different patient groups.**

Gait Modeling, Koopman, DMD, Learned Observables

I. Introduction

The walking gait is a hybrid nonlinear system. It is hybrid because it must switch between two distinct dynamical phases - a swing phase where one foot is in contact with the ground, and a double support phase where both feet are in contact with the floor. Most gait dynamics models must abruptly switch between these two sets of governing dynamic equations once the leading foot makes ground contact. Modeling such switching systems well has proven difficult. Predicting multiple steps of gait requires multiple transitions of diverse dynamic equations, leading to significant prediction error. Here, we present an alternative approach to hybrid dynamic modeling. Koopman Operator has the potential to represent the hybrid, switched nature of gait dynamics as a globally linear, unified dynamic model [1]. No explicit switching would be required for predicting multiple-steps of human gait.

Steady human locomotion requires the seamless interaction of multiple motor and sensory systems to coordinate individual body segments for forward progression while maintaining postural control [2]. For a bipedal system comprised of upper and lower extremity segments pinned at joints with multiple degrees-of-freedom (DoFs), this dual objective of forward translation of the whole-body center of mass (CoM) and dynamic balance requires careful management of body segment rotations. Accordingly, there is compelling evidence that individual segment momenta about the whole-body CoM are coordinated to tightly regulate whole-body angular momentum (WBAM) in all three anatomical axes with each stride [3], both in healthy individuals and when in the presence of musculoskeletal or neurological impairment [4][5]. The phenomenon of regulating WBAM through inter-segmental coordination has even been successfully applied as a control logic for bipedal robots [6][7][8][9], thereby emphasizing the utility and elegance of this locomotor variable in aiding dynamic balance of a multi-DoF system. However, the temporal patterns of WBAM are highly non-linear as they reflect the net effect of multiple body segment momenta around the body CoM [10]. Therefore, given the importance of regulating WBAM to maintain balance while walking, a global linear model of WBAM dynamics would have great utility for analyzing human gait.

Recent successes have been made in the analysis of kinematic and kinetic measures of whole-body motion dynamics modeled in the hidden and cell states of a Recurrent Neural Network (RNN), followed by decomposing phase-averaged projections of the principal components [11]. In that prior work, the system dynamics are captured by the RNN, but the modes found through PCA lack information about their time evolution as it does not explicitly characterize that feature. The gait there is characterized with PCA similar to muscle activation synergies in the biomechanics and motor control community, where a high dimensional feature space is reduced with PCA [12][13][14]. This methodology has shown promise; however, it requires a large amount of data and the resulting model is still nonlinear [11].

To address these limitations, numerical methods have been developed to approximate non-linear and potentially non-periodic dynamics through the Extended Dynamic Mode Decomposition (EDMD) [15]. Both of these numerical methods approximate the Koopman Operator, which linearizes non-linear dynamics by lifting the state space[16]. EDMD utilizes basis functions to lift the state space, including but not limited to radial basis functions, polynomial, trigonometric, machine-learned basis functions, or combinations thereof. Machine learning-derived basis functions have the potential to bypass the manual tuning required by the other methods,

[1]Emily Kamienski and [4]Harry Asada with the Department of Mechanical Engineering, Massachusetts Institute of Technology, 77 Massachusetts Ave., Cambridge, MA 02139, USA emilyk@mit.edu, asada@mit.edu

[2]Seth Donahue with the Motion Analysis Center, Shriners Children's Lexington, 110 Conn Terrace, Lexington, KY 40508, USA Seth.Donahue@shrinenet.org

[3]Matthew J. Major with the Jesse Brown VA Medical Center and Feinberg School of Medicine, Northwestern University, 680 N Lake Shore Drive, Chicago, Illinois 60611, USA matthew-major@northwestern.edu

while also minimizing the number of basis functions required to achieve the same or higher accuracy [17]. Here we explore the use of a Neural Network to learn the dynamics and generate synthetic observables to extend the state space. These observables are algebraic functions of the original state, and do not capture the system dynamics alone.

The eigenvectors and eigenvaleus comprising the modes come directly from the linear state transition matrix. These modes are spatio-temporal modes, where the eigenvectors represent the spatial component and the temporal behavior is determined by the eigenvalues. In this case, the time evolution is in the linear dynamical space, which is distinct from the neural network feature extraction.

Through this technique no manual data interventions are needed as in prior works, such as regularizing to a single phase. The periodicity of the system is identified through the analysis. Furthermore, the model representation is global, and switching between different dynamics is not needed.

The objective of the current work is to apply the Koopman operator method to the modeling and analysis of human gait described in terms of WBAM. We aim to represent the hybrid, switched nature of gait dynamics as a globally linear model in which no explicit switching of governing dynamics is required. Once the human gait dynamics is represented as a linear model in a lifted space, a wealth of linear systems theory and dynamic analysis tools can be applied. These include modal decomposition, spatiotemporal analysis, and frequency-domain analysis. Linear models also facilitate control system design. Model-Predictive Control (MPC), for example, can be applied in a simple, straightforward manner compared to nonlinear MPC.

Despite the salient features, constructing a globally valid Koopman model requires an elaborate methodology. First, finding an effective set of observables remains a challenge. Second, the time horizon where a Koopman model can provide accurate prediction is limited. Often, Koopman models contain unstable poles, which tend to deviate predicted trajectories from the true trajectories in a short time. This does not allow the Koopman model to predict a gait trajectory over a long period of time. Specifically, it is unable to cover multiple steps of gait, which includes repeated switching of governing dynamics. This paper aims to solve this short time-horizon problem, so that a Koopman linear model can predict multiple-steps of gait dynamics. An effective regularization method is presented and applied to the gait dynamics.

Here we estimate linear mode content of steady human walking for comparing young healthy individuals with and without one arm bound. We expect that WBAM will be tightly regulated and constrained within a narrow range and that EDMD analysis will reveal linear modes that define WBAM for the purpose of characterizing individual gait signatures of an aggregate variable describing balance, and provide insight into how bipedal dynamic balance as a control scheme can be modelled through linear modes.

The key contributions are as follows:

1) Create a linear dynamic model of human gait dynamics (WBAM) using the Koopman Operator theory
2) Introduce a regularization term into the loss term for learning the observables for accurately modeling periodic dynamics
3) Characterize the system dynamic modes in terms of spatial and temporal components, creating a new form of gait signature
4) Use this new gait characterization of WBAM dynamics for different cohorts, validating that it must be a highly regulated for stable bipedal walking to occur

II. Koopman Operator Review

In this section, we provide a brief overview of the Koopman Operator and the EDMD for obtaining an approximation of the Koopman operator from data. First we consider the discrete-time dynamical system.

$$x_{t+1} = f(x_t). \tag{1}$$

where $x \in R^n$ is the independent state variable vector representing the system, f is a nonlinear self map function $f : R^n \to R^n$, and t is the current time step. Also consider a real-valued nonlinear output function of the state variables, $g : R^n \to R$, which is called an observable. The Koopman Operator is an infinite-dimensional linear operator acting on the observable function g [16].

$$(\mathcal{K}g)(x) = g(f(x)) \tag{2}$$

where the Koopman Operator $\mathcal{K}$ is linear even though the dynamics of the system are nonlinear.

To obtain a finite-dimensional Koopman Operator from data, the original state vector is augmented with a finite number of observables. Collectively, the augmented state vector $z \in R^m$ is formed

$$z_t = \begin{bmatrix} x_t \\ g_{n+1}(x_t) \\ g_{n+2}(x_t) \\ \vdots \\ g_m(x_t) \end{bmatrix} \tag{3}$$

where m is the order of the lifted state space, corresponding to the number of observable functions, which include the independent state x_t as the first n components. According to the Koopman Operator theory, the time evolution of the lifted state z_t can be represented by:

$$z_{t+1} = Az_t. \tag{4}$$

where $A \in R^{m \times m}$ is a linear operator that evolves the process to the next time step z_{t+1}.

The matrix A is to take as the last linear layer of the network used to obtain the observables.

III. Koopman Modeling of Human Gait Dynamics

This section describes how the Koopman Operator method is applied to human gait modeling based on WBAM. The WBAM vector H consists of 3 components describing the

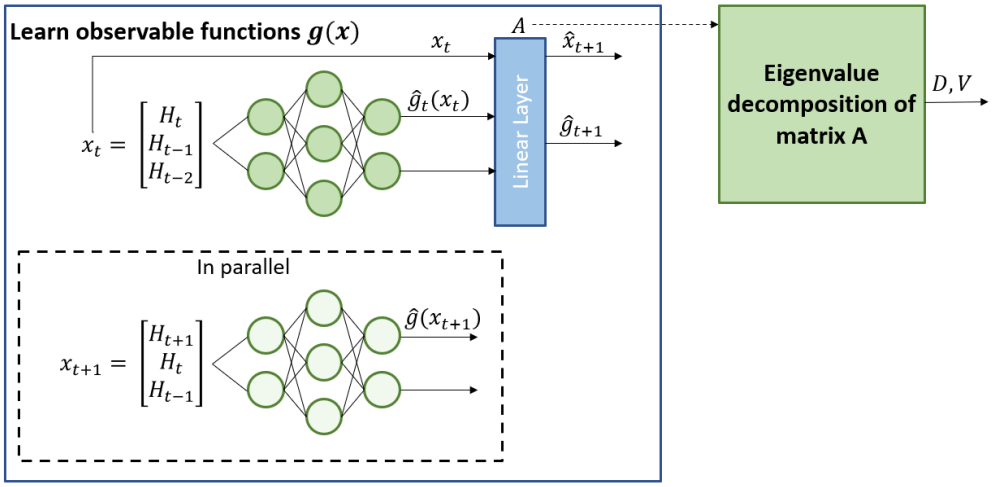

Fig. 1. Observables are learned using a neural network. The last linear layer of the network is taken as the A matrix. Modal analysis is performed on the resulting A matrix, producing eigenvectors and eigenvalues which characterizes the gait spatially and temporally. The left out test data is then used to compute the mode power, indicating the contribution of each mode in that particular data trajectory.

angular momenta about the three orthogonal axes in a human reference frame (sagittal, coronal, and transverse-planes).

$$H_t = \begin{bmatrix} H_x \\ H_y \\ H_z \end{bmatrix} \tag{5}$$

As in [18][19], the state vector, x_t, at time t, that locates the dynamic state of the human gait is given by multiple-time delay embeddings over a time window of length l.

$$x_t = \begin{bmatrix} H_t \\ H_{t-1} \\ H_{t-2} \\ \vdots \\ H_{t-l} \end{bmatrix} \tag{6}$$

Time delay embeddings consist of past states and implicitly provide information as to the recent past evolution of the state. Here it was found that 2 time delay embeddings offered the best prediction accuracy.

Observables were learned by training a neural network, as in [17]. The state vector at the current time step x_t is fed forward in the network so that when combined with the observables output from the observables function, $g_{(x_i)}$, it forms the augmented state. This augmented state is then input into the final linear layer to get the predicted augmented state at the next time step, as illustrated in Fig. 1.

The loss function used in training the observable functions is given by:

$$\begin{aligned} L &= L_{state} + \alpha L_{obs.} \\ &= \frac{1}{n}\sum_{k}^{n} \|x_{k+1} - \hat{x}_{k+1}\|^2 + \alpha \frac{1}{n}\sum_{k}^{n} \|g(x_{k+1}) - \hat{g}_{k+1}\|^2 \end{aligned} \tag{7}$$

Additionally, α is a weight on the observable loss term. Alpha starts at 0 and is linearly increased to 2 with each training epoch. The observable "ground truth" value is expected to be very inaccurate at the start of training since the network weights are changing the most. More emphasis is placed on this loss term as training progresses and there are smaller weight changes.

A. Regularization Term to Enforce Periodicity

We also incorporate domain knowledge for this system when learning the observables. Specifically, we exploit the fact that angular momentum must be conserved. This means that the state transition matrix must be orthonormal for the state, angular momentum, to be conserved.

If

$$AA^T = I \tag{8}$$

then all eigenvalues are on the unit circle.

The proof is as follows. Eq.(8) implies that A is non-singular and $A^T = A^{-1}$. Let λ and W be eigenvalue and eigenvectors of matrix A.

$$AW = \lambda W \tag{9}$$

Taking the squared norm yields,

$$\|AW\|^2 = \|\lambda W\|^2 \tag{10}$$

$$W^T A^T A W = \|\lambda\|^2 W^T W \tag{11}$$

From (8), $W^T A^T A W = W^T W$. Therefore,

$$\|\lambda\|^2 = 1 \tag{12}$$

Thus, all eigenvalues have a magnitude of 1 and are located on the unit circle as in Fig. 2. The regularization term below is added to the loss function during training of the observables to help enforce this constraint.

$$L_{ortho.} = \|AA^T - I\| \tag{13}$$

This regularization term has been used in the computer science community such as in Neural photo editing [20]

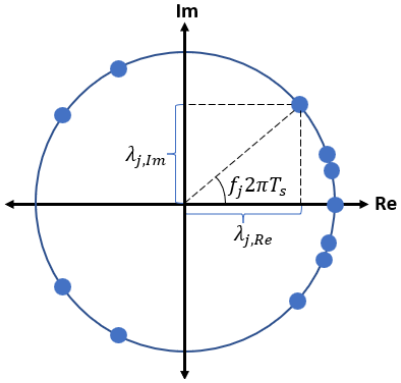

Fig. 2. If (8) is satisfied, then all the eigenvalues are on the unit circle, implying that only periodic modes are found.

but, to the author's knowledge, it has never been used for obtaining periodic modes in Koopman modeling.

If we use the regularization term defined in (13) then periodic modes are obtained.

Thus, the resulting loss function is given by

$$L = L_{state} + \alpha L_{obs.} + \beta L_{ortho.} \tag{14}$$

where β is another tunable weight. If a significantly large weighting factor β is used, then all eigenvalues will be on the unit circle.

B. Modal Decomposition

Now that the linear Koopman model is obtained, we want to characterize human gait based on linear modal analysis. First, the state transition matrix A is decomposed to eigen modes.

$$A = VDV^{-1} \tag{15}$$

where $D = diag.(\lambda_1, \ldots, \lambda_m)$, with the eigenvalues λ_i of matrix A, the matrix V consists of the corresponding eigenvectors v_i, and its inverse matrix is written as,

$$V^{-1} = \begin{bmatrix} \tilde{v}_1 \\ \tilde{v}_2 \\ \vdots \\ \tilde{v}j \\ \vdots \\ \tilde{v}_m \end{bmatrix} \tag{16}$$

This allows us to examine the time evolution of each mode separately. The i-th mode is given by

$$\tilde{v}_i z_{t+1} = \lambda_i \tilde{v}_i z_t, i = 1, \ldots, m \tag{17}$$

To quantify the signal strength of each mode, consider the squared magnitude,

$$|\tilde{v}_i z_{t+1}|^2 = |\lambda_i|^2 |\tilde{v}_i z_t|^2, \tag{18}$$

We are particularly interested in those periodic modes having the eigenvalues on the unit circle, $|\lambda_j| = 1$,

$$|\tilde{v}_i z_{t+1}|^2 = |\tilde{v}_i z_t|^2, \tag{19}$$

This implies that the power of each periodic mode is preserved through time. To evaluate the significance of each periodic mode in experimental data, we characterize it by taking the average power of each periodic mode over the experimental data.

$$\phi_j = \frac{1}{N} \sum_{k=0}^{N-1} |\tilde{v}_j z_k|^2 \tag{20}$$

Taking the summation over each subject group, we can compare those subject groups in terms of the power of periodic modes. The frequencies can be directly compared with the eigenvalues. The frequency is calculated by

$$f_j = \frac{1}{2\pi T_s} \arctan(\frac{\lambda_{Im,j}}{\lambda_{Re,j}}) \tag{21}$$

where T_s is the sampling frequency.

IV. Experiments

A. Data

In the current analysis, existing data from 10 participants were used, which originated from two previous projects at the Northwestern University Prosthetics-Orthotics Center. Both were approved by the Jesse Brown VA Medical Center IRB under protocols #1569928 and #1462955. Data from two groups are used: 1) able-bodied (AB) healthy adults (at least 18 years old) with both arms free to swing (n_1 = 5), 2) the same able-bodied adults as in group (1) but with one arm bound to the torso (AB bound) to restrict arm swing (n_2 = 5).

All participants were able to walk for 5 minutes or more without fatigue. Any conditions or medication use affecting balance restricted participation.

B. Experimental Protocol

All participants completed a single trial on an instrumented treadmill (Motek, Enschede, Netherlands). The trial consisted of 30 seconds of steady-state walking at 1.0 m/s. Body segment mass, *I* and COM location were estimated using established regression equations for biomechanical modelling [21]. Kinematic data of a full-body marker set attached to body landmarks [22] were collected with a 12-camera optical motion capture system (Motion Analysis Corp., Rohnert Park, CA) at 120 Hz, Data were then exported to Visual 3D (C-Motion, Germantown, MD) for filtering with a 4^{th} order low-pass (9Hz) Butterworth filter and application of a personalized 12-segment biomechanical model [22]. From these data, limb initial contacts and toe off events were labelled with a velocity-based algorithm [23] and then corrected manually if necessary. WBAM, or *H*, was estimated by calculating the instantaneous angular momentum of each segment about itself and the whole-body COM in all three planes of motion and summing the values according to eq. 22.

$$H = \sum_{i=1}^{n} I_i \omega_i + r_i \times m_i v_i \tag{22}$$

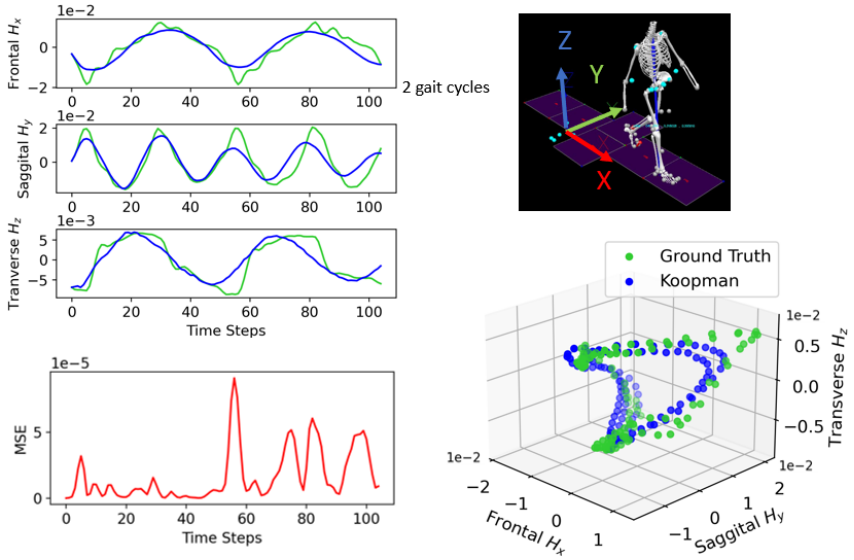

Fig. 3. Example prediction over 2 gait cycles for able-bodied subject 4 with both arms free to swing. Given the initial H measurement, the dynamics were propogated forward with the matrix A found by taking the last linear layer of the trained network. Top-right illustrated the reference frame defining the H orthogonal components.

H was normalized by treadmill speed and the height and mass of the participant. For each segment i, I_i was the moment of Inertia, ω_i was the angular velocity, r_i, was the distance from the segment COM to the whole-body COM. The mass of each segment was defined as m_i and the relative velocity of the segment to the whole-body COM was v_i. The calculated whole body angular momentum values were down sampled to 40 Hz for constructing the model.

C. Learning Observable Functions

Models were trained for individual subjects on 30 seconds of data obtained during steady walking. A 70%-15%-15% train-validation-test split was used. Data samples input to the neural network consisted of WBAM, H, and H at the previous two time steps, or two time embeddings. Two time embeddings resulted in the best accuracy of those tested. Likewise, 16 observables were found to produce accurate models.

The loss function was mean squared error (MSE) and took the form mentioned earlier in eq. 14 and the optimizer was ADAM. The parameters for the neural network may be found in Table A1 in the appendix.

D. Prediction with Linear Dynamic Model

The last linear layer of the trained neural network was taken as the state transition matrix A. Given an initial measurement corresponding to left heel contact, eq. 4 was used to propagate the system through 2 full gait cycles, defined as left foot initial contact to the next initial contact of the ipsilateral limb. The mean squared error at each time step t was calculated for the three predicted angular momentum components.

$$E_{mse,t} = \frac{1}{3}\|H_t - \hat{H}_t\|^2 \tag{23}$$

where the estimated angular momentum $\hat{H}$ is the prediction from the model and the ground truth is denoted as H.

V. Results

A. Prediction Accuracy

Fig. 3 shows the prediction accuracy for one able-bodied subject for 2 gait cycles when $\beta = 0.1$. We observed that accurate models were produced for most individual subjects.

The MSE over 2 gait cycles for both groups are shown in Fig. 6 for 5 trials per group type when $\beta = 0.1$. A different person performed each trial in a group. The solid line represents the average mean-squared error across the 5 trials and the shaded region shows the range of the error. Fig. 6 shows that good prediction accuracy may be obtained over 2 gait cycles for varying gait dynamics for subjects in the able-bodied and able-bodied bound groups. We will now discuss how $\beta = 0.1$ was found to produce the most accurate models for these groups.

B. Regularization Term Effect

Fig. 4 shows the impact of the regularization term on the resulting eigenvalues of the state transition matrix A, and the prediction accuracy. When there is no regularization term, when $\beta = 0.0$, it is possible to have unstable poles, as in the top pole plot in Fig. 4. When the orthonormal regularization term is too small, when $\beta = 0.01$, there is a pair of poles corresponding to the saggital plane base frequency that is not on the unit circle. The result is that the sagittal plane signal decays, as seen in the middle of Fig. 4. When the orthonormal regularization term is added in with sufficient weight, the poles are pushed onto the unit circle, eliminating the artificial signal decay.

Fig. 5 shows the aggregate error results for all 5 subjects for each subject group as a function of β, the weight on the

orthonormal regularization term. Note that the error without the orthonormal regularization term, when $\beta = 0$, was left out since there were unstable poles in these cases, and sometimes very high errors. $\beta = 0.01$ and $\beta = 0.1$ produced the lowest errors on average for all two subject groups.

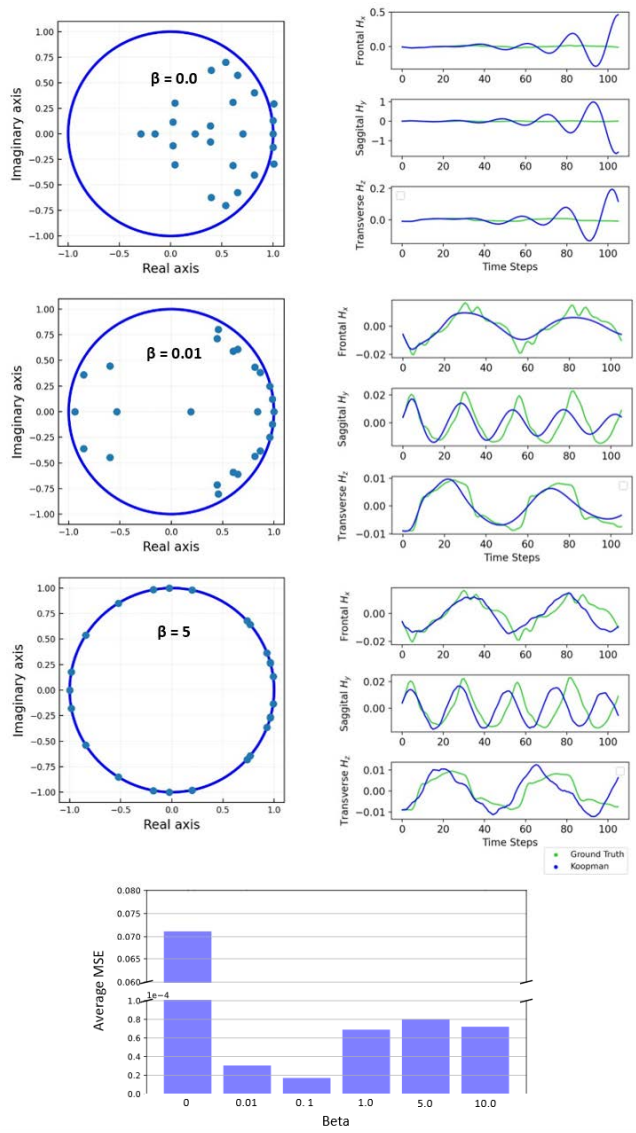

Fig. 4. Eigenvalue plots and model prediction over 2 gait cycles with different values of β, or weighting on the orthonormal regularization term, for a single able-bodied subject with one arm bound (top). β = 0 corresponds to no regularization term. Increasing β pushes the poles towards the unit circle. The average MSE across the 2 gait cycles for each value of β tested is shown (bottom). β = 0.01 gave the most accurate prediction.

C. Eigenmodes

Fig. 7 shows the average eigevector mode power, ϕ_i for the largest 3 modes for each subject group. For the high accuracy models, the first 2 modes have eigenvalues equal to 1, corresponding to the periodic modes. The first mode, ϕ_1 generally corresponds to the base frequency of H in the frontal and transverse planes, H_x and H_z, respectively, as calculated in eq. 21. The frequency of the second most

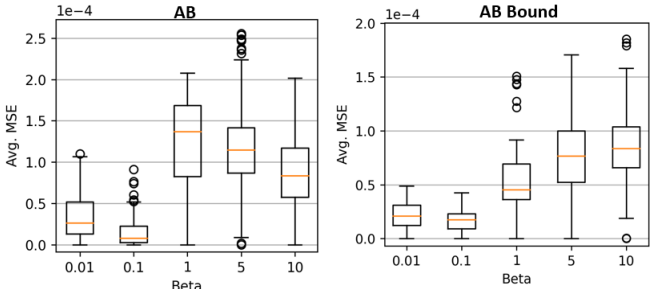

Fig. 5. Aggregate error results across all 5 able-bodied subjects for different values of β, the weighting factor on the orthonormal regularization term. Not shown is that the error is significantly higher without the regularization term due to unstable poles in some of the models (when $beta = 0$). The values of β that produced the lowest error were 0.01 and 0.1.

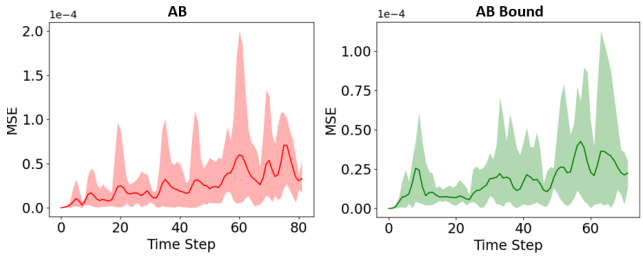

Fig. 6. The mean squared error (MSE) of the Koopman model prediction over 2 gait cycles for each population when $\beta = 0.1$. The solid line is the average MSE of the prediction when the initial point is taken over 2 gait cycles. The shaded region represents the range of the MSE error of each trajectory at each timestep.

active mode corresponds with the base frequency of H in the saggital plane, H_y. The other modes mostly help capture the more subtly higher frequency components of the signal.

The mode power, or eigenvector activation, is fairly consistent between the able-bodied and able-bodied bound group, which consist of the same subjects. There is a slight redistribution of the activation of the first and second modes as the average activation of the first mode increases slightly and the second mode decreases a little. The bounded arm may be the cause of this difference.

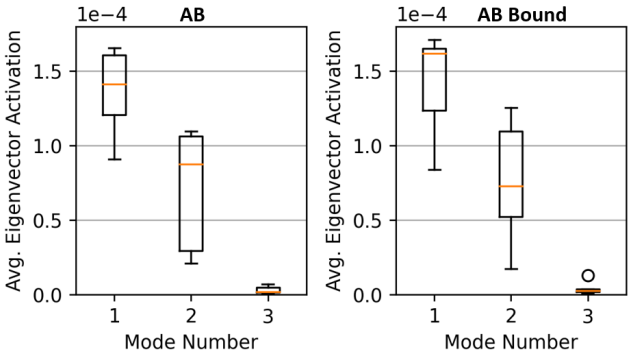

Fig. 7. Eigenvector activations or mode powers during 5 trajectories per subject group for the 3 most active eigenvector modes. $\beta = 0.1$.

VI. Discussion

Here we demonstrate the success of using EDMD and Koopman Operators to model the human walking behavior that is reflective of dynamic balance in bipedal gait. This technique allowed expression of the spatial and temporal linear mode content of these non-linear dynamics with high accuracy. Our orthonormal regularization term was effective in pushing decaying poles onto the unit circle so that the periodic dynamics could be adequately captured. This technique can also be applied to non-periodic systems, as this regularization term is also a method to address the occurence of unstable poles, a common problem when learning observable functions.

The poles in the complex plane can quickly show the behavior of the constructed model's modes. Complex poles along the perimeter of the unit circle indicate oscillatory motions, and their magnitude indicates the frequency of these oscillations. This is expected as angular momentum is periodic during the gait cycle. Poles outside the unit circle indicate unstable modes, which means that the predicted H will diverge from the true H. Poles inside the unit circle indicate that these modes will decay to zero. It would be expected for steady walking that most of the poles lie along the unit circle, to represent the superposition of different frequencies.

A potential limitation of this work is that it assumes that the human steady walking can be modeled as an autonomous system. Participant differences as step-to-step variability as related to the body system and neuromotor control may play a significant role. However, here we have examined H, which is a tightly regulated variable, in groups with physical impairment but without neurological insult. Future work can include constructing models for other population types and comparing the resulting mode activations. The activations of the most prominent modes may be plotted at each point in time over a trajectory to show the spatial representation of the signal evolve over time. While we have characterized the dynamics of human gait, our technique could be translated to modeling the control scheme of robotic bipedal gait when aiming to maintain upright postural control during forward progression via intersegmental angular momentum cancellation. As regulation of H in human biological gait is demonstrated across different types of ambulatory scenarios to facilitate stable gait, the linear mode characterization presented here could offer insight into a generalized control scheme for robotic bipedal gait.

VII. Conclusion

This work presented a method for creating a linear dynamic model of human balance while walking, in the form of whole body angular momentum. This was enabled through the use of Koopman Operators and the accuracy was improved through the use of an orthonormal regularization term. This method was demonstrated on steady walking data from 2 different groups. Models were constructed for individuals from each group and good accuracy was achieved over 2 gait cycles for both groups. Modal analysis may be performed on the resultant linear models, which allows a comparison of different subject types.

Appendix I

TABLE A1
NN parameter values

# Dense Layers	4
# Dense Hidden Units	16
Learning rate	1e-3
Batch size	5

Acknowledgment

This work was supported in part by the National Robotics Initiative (NSF-2133072), the National Science Foundation (NSF-CMMI 2021625) and by the U.S. Department of Veterans Affairs (grants 1IK2RX001322 and I21RX003290, PI M.J. Major). The manuscript contents do not represent the views of the U.S. Department of Veterans Affairs or the United States Government.

References

[1] H. H. Asada, "Global, unified representation of heterogenous robot dynamics using composition operators: A koopman direct encoding method," *IEEE/ASME Transactions on Mechatronics*, vol. 28, no. 5, pp. 2633–2644, 2023.

[2] K. Takakusaki, "Functional neuroanatomy for posture and gait control," *Journal of Movement Disorders*, vol. 10, no. 1, pp. 1–17, Jan. 2017.

[3] H. Herr and M. Popovic, "Angular momentum in human walking," *Journal of Experimental Biology*, vol. 211, no. 4, pp. 467–481, 02 2008. [Online]. Available: https://doi.org/10.1242/jeb.008573

[4] G. Hisano, H. Murata, T. Kobayashi, M. J. Major, M. Nakashima, and H. Hobara, "Dynamic balance during walking in transfemoral prosthesis users: Step-to-step changes in whole-body and segment angular momenta," *IEEE Transactions on Neural Systems and Rehabilitation Engineering*, vol. 31, pp. 2893–2902, 2023.

[5] J. A. Kent and M. J. Major, "Asymmetry of mass and motion affects the regulation of whole-body angular momentum in individuals with upper limb absence," *Clinical Biomechanics*, vol. 76, no. August 2019, p. 105015, 2020, publisher: Elsevier. [Online]. Available: https://doi.org/10.1016/j.clinbiomech.2020.105015

[6] S.-H. Lee and A. Goswami, "A momentum-based balance controller for humanoid robots on non-level and non-stationary ground," *Autonomous Robots*, vol. 33, 11 2012.

[7] S. Kajita, F. Kanehiro, K. Kaneko, K. Fujiwara, K. Harada, K. Yokoi, and H. Hirukawa, "Resolved momentum control: Humanoid motion planning based on the linear and angular momentum," vol. 2, 11 2003, pp. 1644 – 1650 vol.2.

[8] D. Orin, A. Goswami, and S.-H. Lee, "Centroidal dynamics of a humanoid robot," *Autonomous Robots*, vol. 35, 10 2013.

[9] H. Dai, A. Valenzuela, and R. Tedrake, "Whole-body motion planning with centroidal dynamics and full kinematics," in *2014 IEEE-RAS International Conference on Humanoid Robots*, 2014, pp. 295–302.

[10] H. Herr and M. Popovic, "Angular momentum in human walking," *Journal of Experimental Biology*, vol. 211, no. 4, pp. 467–481, 2008.

[11] T. S. Winner, M. C. Rosenberg, K. Jain, T. M. Kesar, L. H. Ting, and G. J. Berman, "Discovering individual-specific gait signatures from data-driven models of neuromechanical dynamics," *PLOS Computational Biology*, vol. 19, no. 10, pp. 1–33, 10 2023. [Online]. Available: https://doi.org/10.1371/journal.pcbi.1011556

[12] B. L. Davis and C. L. Vaughan, "Phasic behavior of emg signals during gait: Use of multivariate statistics," *Journal of Electromyography and Kinesiology*, vol. 3, no. 1, pp. 51–60, 1993. [Online]. Available: https://www.sciencedirect.com/science/article/pii/105064119390023P

[13] A. E. Patla, T. W. Calvert, and R. B. Stein, "Model of a pattern generator for locomotion in mammals," *American Journal Physiology Regulatory Integrative and Comparative Physiology*, vol. 248, no. 4, pp. R484–R494, Apr. 1985.

[14] R. Ranganathan and C. Krishnan, "Extracting synergies in gait: using EMG variability to evaluate control strategies," *Journal of Neurophysioly*, vol. 108, no. 5, pp. 1537–1544, Sep. 2012.

[15] M. O. Williams, I. G. Kevrekidis, and C. W. Rowley, "A Data–Driven Approximation of the Koopman Operator: Extending Dynamic Mode Decomposition," *Journal of Nonlinear Science*, vol. 25, no. 6, pp. 1307–1346, 2015, publisher: Springer US _eprint: 1408.4408.

[16] B. Koopman, "Hamiltonian systems and transformation in hilbert space," *Proceedings of the National Academy of Sciences of the United States of America*, vol. 17, no. 5, p. 315—318, May 1931.

[17] B. Lusch, J. N. Kutz, and S. L. Brunton, "Deep learning for universal linear embeddings of nonlinear dynamics," *Nature Communications*, vol. 9, no. 1, 2018, _eprint: 1712.09707.

[18] S. M. Hirsh, S. M. Ichinaga, S. L. Brunton, J. Nathan Kutz, and B. W. Brunton, "Structured time-delay models for dynamical systems with connections to Frenet-Serret frame," *Proc. Math. Phys. Eng. Sci.*, vol. 477, no. 2254, p. 20210097, Oct. 2021.

[19] M. Kamb, E. Kaiser, S. L. Brunton, and J. N. Kutz, "Time-delay observables for koopman: Theory and applications," *SIAM Journal on Applied Dynamical Systems*, vol. 19, no. 2, pp. 886–917, 2020. [Online]. Available: https://doi.org/10.1137/18M1216572

[20] A. Brock, T. Lim, J. Ritchie, and N. Weston, "Neural photo editing with introspective adversarial networks," in *International Conference on Learning Representations*, 2017. [Online]. Available: https://openreview.net/forum?id=HkNKFiGex

[21] D. A. Winter, *Biomechanics and motor control of human movement*. Hoboken, NJ, USA: John Wiley & Sons, Inc., Sep. 2009.

[22] J. A. Kent and M. J. Major, "Asymmetry of mass and motion affects the regulation of whole-body angular momentum in individuals with upper limb absence," *Clinical Biomechanics*, vol. 76, no. August 2019, p. 105015, 2020. [Online]. Available: https://doi.org/10.1016/j.clinbiomech.2020.105015

[23] J. A. Zeni, J. G. Richards, and J. S. Higginson, "Two simple methods for determining gait events during treadmill and overground walking using kinematic data," *Gait and Posture*, vol. 27, no. 4, pp. 710–714, 2008.